Indian Journal of Chemistry
Vol. 59A, April 2020, pp. 533-550

Phosphorus-nitrogen compounds. Part 48. syntheses of the phosphazenium salts containing 2-pyridyl pendant arm: structural characterizations, thermal analysis, antimicrobial and cytotoxic activity studies

Gamze Elmas[a,*], Aytuğ Okumuş[a,*], Zeynel Kılıç[a], Pelin Özbeden[b], Leyla Açık[b], Beste Çağdaş Tunalı[c], Mustafa Türk[c], Nebahat Aytuna Çerçi[b] & Tuncer Hökelek[d]

[a]Department of Chemistry, Ankara University, Ankara 06100, Turkey

[b]Department of Biology, Gazi University, Ankara 06500, Turkey

[c]Department of Bioengineering, Kırıkkale University, Yahşihan-Kırıkkale 71450, Turkey

[d]Department of Physics, Hacettepe University, Ankara 06800, Turkey

Email: gegemen@ankara.edu.tr (G E)/ okumus@science.ankara.edu.tr (A O)

Received 28 June 2019; revised and accepted 12 March 2020

The phosphazenium salts (protic ionic liquids, PILs/protic molten salts, PMOSs) (**6a-6d** and **7a**) of the free phosphazene bases (**4a-4d** and **5a**) have been prepared by the reactions of the corresponding cyclotriphosphazenes with the bulky gentisic acid. The structures of the PMOS have been evaluated using the elemental analyses, FTIR, ^{1}H, $^{13}C\{^{1}H\}$ and $^{31}P\{^{1}H\}$ NMR data. The molecular and crystal structures of **4a** and **6c** are established by X-ray crystallography. The thermal properties of the PMOS are determined using TG and DTA techniques. On the other hand, the antimicrobial activities of the free phosphazene bases (**4a-4d** and **5a-5d**) and PMOSs (**6a-6d** and **7a**) are screened against the selected bacteria and yeast strains. The antimicrobial activities of the free phosphazene bases and the PMOSs are compared. The interactions of the phosphazenes and their salts with plasmid DNA are elucidated by the agarose gel electrophoresis. The evaluations of the cytotoxic activities of these compounds are also studied against to L929 fibroblast and breast cancer cells (MDA-MB-231).

Keywords: 2-Pyridylspirocyclotriphosphazenes, Phosphazenium salts (PMOSs), Thermal analysis, Cytotoxicity

Hexachlorocyclotriphosphazene, $N_3P_3Cl_6$ (**1**) has six very reactive P-Cl bonds, and it is a well-known starting compound for preparation of numerous trimeric and polymeric organophosphazene derivatives.[1,2] The replacement reactions of $N_3P_3Cl_6$ with a large number of mono-, di-, tri- and tetradentate reagents led to the formation of the partly and/or fully substituted trimeric phosphazene derivatives.[3-8] The pendant armed monospirocyclotriphosphazene derivatives are very rare,[9,10] and they have four reactive P-Cl bonds available for the syntheses of tetra-substituted organophosphazenes.[11,12] A number of organocyclotriphosphazenes are used to liquid crystals,[13,14] ionic liquids,[15,16] organic light emitting diodes (OLEDs),[17,18] Li-ion batteries,[19] fluorescence sensors[20] and biomaterials.[21] The cyclophosphazenes are also used as antimicrobial agents against some bacteria and yeast strains,[22,23] and as anticancer agents against various cancer cell lines.[24,25]

The fully amino and alkylamino substituted cyclotriphosphazenes ought to be used as the potential phosphazene bases. The values of pKa′ of some organocyclotriphosphazenes were presented in the literature.[26] The strong phosphazene bases can form stable monoprotonated salts with inorganic and organic acids such as HCl, HF, $HClO_4$ and CH_3COOH.[27] In recent years, several papers have been published about the pendant armed phosphazenium salts with bulky organic acids. These salts may occur by proton transfer from Brønsted acid to Brønsted base (for instance; free phosphazene base), and they can be termed as protic molten salts (PMOSs).[28-31] These salts can also be defined as protic ionic liquids (PILs) at the same time. Phosphazenium salts (PMOSs or PILs) are soluble in various organic apolar/polar solvents and dissoluble slightly in water. Since, in biological studies the solubilities in the biological fluids are so crucial, the investigation of antimicrobial and cytotoxic activities of the PMOSs may be quite important and useful for future studies. However, the antibacterial, antifungal[28-31] and anticancer activity[30,31] studies of phosphazenium salts

are also very rare. Furthermore, thermal analysis studies are used to determine the thermal properties of the cyclotriphosphazenes and their salts, PMOSs/PILs.[29-31] The data obtained from these measurements may be useful to determine whether PMOSs are likely to be used as ionic liquids.

In the last two decades, several chiral cyclophosphazene derivatives were synthesized and the chiralities of these products were investigated using X-ray crystallography, HPLC and/or ^{31}P NMR spectroscopy on the addition of (R)-(+)-2,2,2-trifluoro-1-(9'-anthryl)-ethanol (CSA).[32-34] However, there is no study published in the literature about the determination of the chiral properties of the phosphazenium salts by X-ray crystallography. In this study, the protic molten salts (PMOSs; **6a-6d** and **7a**) were prepared from the reactions of the fully substituted phosphazene bases (**4a-4d** and **5a**) with the gentisic acid for the assessment of their structural, stereogenic and thermal properties, and antibacterial, antifungal and cytotoxic activities.

Materials and Methods

Reagents

The solvents and reagents were purified and dried using conventional methods before use. $N_3P_3Cl_6$ (Aldrich), pyridine-2-carboxaldehyde (Merck), N-methylpropane-1,3-diamine (Merck), 3-amino-1-propanol (Merck), pyrrolidine (Fluka), piperidine (Fluka), morpholine (Fluka), DASD (Fluka) and 2,5-dihydroxybenzoic acid (Merck) were supplied. The free phosphazene bases (**4a-4d** and **5a-5d**) were prepared according to reported procedures.[35,36]

Measurements

The Cl exchange reactions were carried out under Ar atmosphere, and they were followed by thin-layer chromatography (TLC) on Merck DC Alufolien Kiesegel 60 B_{254} sheets. The column chromatography was performed on Merck Kiesegel 60 (230–400 mesh ATSM) silica gel. The melting points of the compounds were determined with a Gallenkamp apparatus using a capillary tube. Electron spray ionization-mass spectrum (ESI-MS) of **5a** was detected on the AGILENT 1100 MSD mass spectrometer. The Fourier transform infrared (FTIR) spectra were recorded on a Jasco FT/IR-430 spectrometer in KBr discs and reported in cm^{-1} units. ^{1}H, ^{13}C, and ^{31}P NMR spectra were monitored on a Bruker DPX FT-NMR (500 MHz) spectrometer ($SiMe_4$ as internal and 85% H_3PO_4 as external standards), operating at 400.13, 100.62 and 242.93 MHz. The NMR spectrometer was equipped with a 5 mm PABBO BB inverse gradient probe and standard Bruker pulse programs[37] were used. Microanalyses were realized by the microanalytical service of Ankara University. Thermal stabilities and decomposition features of the PMOS were evaluated using thermogravimetric (TG)-differential thermal analysis (DTA). TG and DTA curves were scanned by a PYRIS Diamond TG/DTA apparatus in N_2 (platinum crucibles, heating rate: 10 °C/min, mass ~10 mg and temperature range 35-1150 °C).

Single crystal X-ray structure determinations

The colorless crystals of **4a** and **6c** were crystallized from toluene at ambient temperature. The crystallographic details of these compounds were listed in Table 1. Crystallographic data of **4a** and **6c** were recorded on a Bruker Kappa APEXII CCD area-detector diffractometer using Mo K_α radiation (λ = 0.71073 Å) at T = 120(2) K. Absorption correction by multi-scan[38] was applied. The structures were solved by direct methods and refined by full-matrix least squares against F^2 using all data.[39,40] All non-H atoms were refined anisotropically. The molecular and packing diagrams together with the

Table 1 — Crystallographic Details for **4a** and **6c**

	4a	**6c**
Empirical Formula	$C_{29}H_{52}N_9OP_3$	$C_{32}H_{50}N_9O_9P_3$
Fw	635.71	797.72
Crystal System	triclinic	triclinic
Space Group	*P -1*	*P -1*
a (Å)	9.4852(3)	11.0344(3)
b (Å)	10.2984(3)	11.8558(3)
c (Å)	17.641(4)	15.9041(4)
α (°)	81.895(3)	72.367(3)
β (°)	89.865(4)	88.550(4)
γ (°)	77.058(3)	72.352(3)
V (Å^3)	1661.9(4)	1884.45(8)
Z	2	2
μ (cm^{-1})	0.71073 (Mo K_α)	0.71073 (Mo K_α)
ρ (calcd) (g cm^{-3})	1.270	1.406
Number of Reflections Total	5843	6642
Number of Reflections Unique	5207	4600
R_{int}	0.0488	0.0691
$2\theta_{max}$ (°)	50.06	50.06
Number of Parameters	379	482
R [$F^2 > 2\sigma(F^2)$]	0.0640	0.0831
wR	0.1387	0.1279

ring conformations were drawn by the ORTEP-3 program incorporated into the WinGX package. The C-bonded H atoms were positioned geometrically at distances of 0.93 Å (CH) and 0.97 Å (CH_2) from the parent C atoms; a riding model was used during the refinement process and the U_{iso}(H) values were constrained to be $1.2U_{eq}$(carrier atom).

General procedure for the syntheses of the free phosphazene base (5a) and PMOSs (6a-6d and 7a)

Synthesis of 2-pyridyl(N/N)spirotetrapiperidino-cyclotriphosphazene (5a)

N-(2-Pyridyl)-methyl-*N'*-methylpropane-1,3-diamine (**3**) was synthesized from the reactions of pyridine-2-carboxyaldehyde with *N*-methylpropane-1,3-diamine in ethanol at −10 °C, as described in the literature.[41] The Cl substitution reaction of $N_3P_3Cl_6$ with **3** gave the partly substituted 2-pyridyl(N/N) spirocyclotriphosphazene (**5**) (with a yield of 57%) in dry THF according to the published paper.[35] A solution of **5** (0.80 g, 1.80 mmol) and triethylamine (1.00 mL, 7.20 mmol) in dry THF (100 mL) was added slowly to a solution of piperidine (1.42 mL, 14.40 mmol) in dry THF (50 mL) under Ar atmosphere. The mixture was stirred for 2 days at ambient temperature, and then it was refluxed for 3 days. The crude product was purified by column chromatography using toluene-THF (3:1) as eluent. A colorless powder of **5a** was crystallized from toluene. Yield: 0.74 g (63%). M.P.: 155 °C. Anal. Calcd. for $P_3N_{10}C_{30}H_{55}$. 0.5 C_7H_8, 694.40 g/mol: C, 57.98; H, 8.57; N, 20.18. Found: C, 57.64; H, 8.28; N, 20.02. ESI-MS (Ir %): *m/z* 649 ($[M+H]^+$, 100). FTIR (KBr, cm^{-1}): *ν* 2962, 2848 (C-H aliph.), 1253 (asymm.), 1151 (symm.) (P=N). ^{1}H NMR (400 MHz, $CDCl_3$, ppm, in Scheme 1 the numberings of protons were given): *δ* 8.48 (d, H, $^3J_{HH}$=4.4 Hz, H_5), 7.72 (d, H, $^3J_{HH}$=7.2 Hz, H_2), 7.63 (dd, H, $^3J_{HH}$=7.2 Hz, $^3J_{HH}$=7.6 Hz, H_3), 7.11 (dd, H, $^3J_{HH}$=6.2 Hz, $^3J_{HH}$=6.2 Hz, H_4), 4.11 (d, 2H, $^3J_{PH}$=7.2 Hz, Py-CH_2-N), 3.16 (m, 2H, CH_3-N-CH_2), 3.01 (m, 2H, Py-CH_2-N-CH_2), 3.06 [m, 8H, N-CH_2 (piper)], 2.98 [m, 8H, N-CH_2 (piper)], 2.57 (d, 3H, $^3J_{PH}$=13.2 Hz, N-CH_3), 1.80 (m, 2H, N-CH_2-CH_2), 1.48 [m, 16H, N-CH_2-CH_2 (piper)], 1.31 [m, 4H, N-CH_2-CH_2-CH_2 (piper)], 1.28 [m, 4H, N-CH_2-CH_2-CH_2 (piper)]. ^{13}C NMR (100 MHz, $CDCl_3$, ppm, in Scheme 1 the numberings of carbons were given): *δ* 160.92 (d, $^3J_{PC}$=12.3 Hz, C_1), 148.57 (s, C_5), 136.41 (s, C_3), 121.95 (s, C_2), 121.62 (s, C_4), 53.03 (m, Py-*C*H_2-N), 51.00 (s, Py-CH_2-N-*C*H_2), 47.32 (s, *C*H_3-N-CH_2), 45.54 and 45.42 [s, N-*C*H_2 (piper)], 36.54 (m, N-CH_3), 25.50 (s, N-CH_2-*C*H_2), 26.46 and 26.31 [(s, N-CH_2-*C*H_2 (piper)], 25.10 and 24.97 [(s, N-CH_2-CH_2-*C*H_2 (piper)].

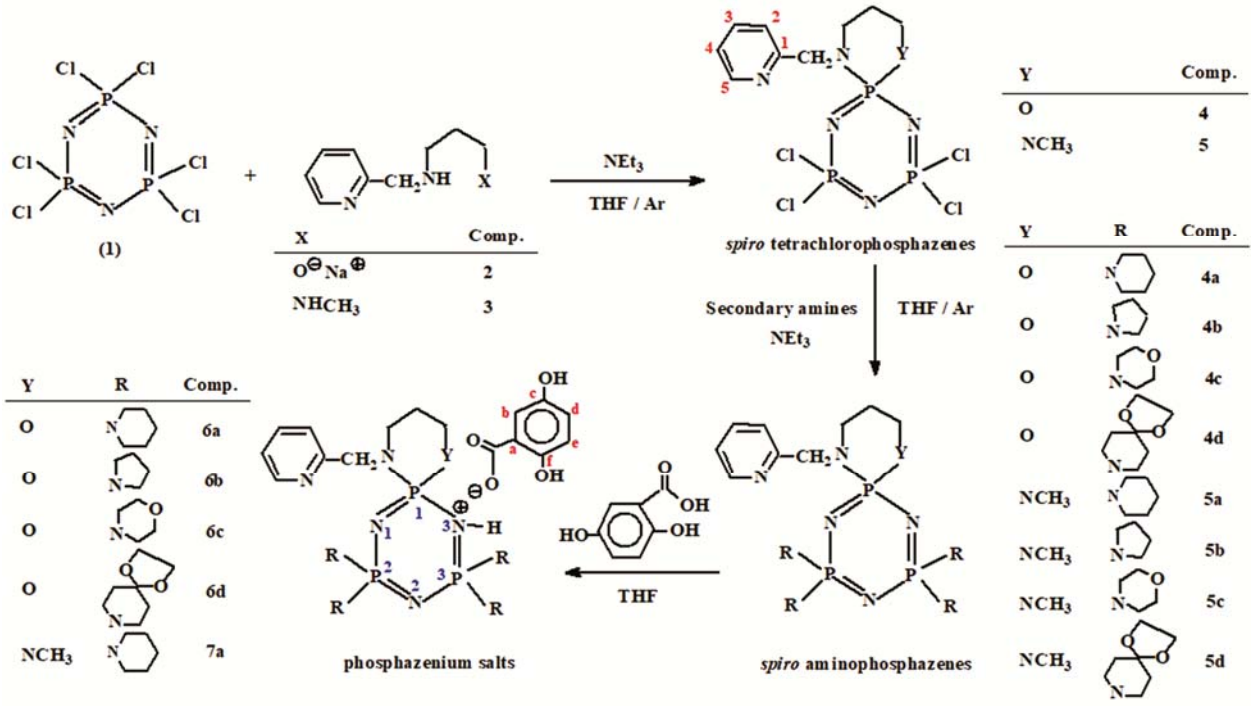

Scheme 1 — Cyclotriphosphazene derivatives are synthesized from the reactions of 2-pyridylspiro(N/O)cyclotriphosphazene with secondary amines and their phosphazenium salts.

Synthesis of 2-pyridyl(N/O)spirotetrapiperidino-PMOS (6a)

A solution of **4a** (0.50 g, 0.79 mmol) in dry THF (30 mL) was slowly added by the dropwise to gentisic acid (0.12 g, 0.79 mmol) in dry THF (10 mL) at the ambient temperature. The reaction mixture was refluxed for over 45 h. After that, the solvent was evaporated under vacuo. A colourless powder of **6a** was crystallized from toluene. Yield: 0.48 g (77%). M.P.: 105 °C. Anal. Calcd. for $P_3N_9O_5C_{36}H_{57} . C_7H_8$, 880.40 g/mol: C, 58.66; H, 7.44; N, 14.33. Found: C, 58.34; H, 7.19; N, 14.16. FTIR (KBr, cm^{-1}): *v* 3195 (O-H), 2919, 2849 (C-H aliph.), 2664 (N^+-H), 1572 (asymm.), 1374 (symm.) (COO^-), 1240 (asymm.), 1194 (symm.) (P=N). ^{1}H NMR (400 MHz, $CDCl_3$, ppm, in Scheme 1 the numberings of protons were given): δ 9.12 (b, 2H, Ar-O*H*), 8.54 (d, H, $^3J_{HH}$=4.0 Hz, H_5), 7.73 (dd, H, $^3J_{HH}$=8.0 Hz, $^3J_{HH}$=7.6 Hz, H_3), 7.66 (d, H, $^3J_{HH}$=7.6 Hz, H_2), 7.55 (d, 1H, $^3J_{HH}$=2.8 Hz, H_b), 7.14 (dd, H, $^3J_{HH}$=7.6 Hz, $^3J_{HH}$=7.6 Hz, H_4), 6.90 (dd, 1H, $^3J_{HH}$=8.8 Hz, $^3J_{HH}$=3.2 Hz, H_d), 6.73 (d, 1H, $^3J_{HH}$=8.4 Hz, H_e), 4.51 (t, H, $^3J_{PH}$=10.8 Hz, $^2J_{HH}$=5.2 Hz, O-CH_2), 4.47 (t, H, $^3J_{PH}$=10.4 Hz, $^2J_{HH}$=5.2 Hz, O-CH_2), 4.28 (d, 2H, $^3J_{PH}$=9.2 Hz, Py-CH_2-N), 3.26 (t, H, $^3J_{PH}$=11.6 Hz, $^2J_{HH}$=4.8 Hz, Py-CH$_2$-N-CH_2), 3.20 (t, H, $^3J_{PH}$=11.6 Hz, $^2J_{HH}$=5.2 Hz, Py-CH$_2$-N-CH_2), 3.07 [m, 8H, N-CH_2 (piper)], 3.01 [m, 8H, N-CH_2 (piper)], 1.93 (m, 2H, $^3J_{HH}$=4.4 Hz, $^3J_{HH}$=5.6 Hz, N-CH$_2$-CH_2), 1.51 [m, 8H, N-CH$_2$-CH_2 (piper)], 1.44 [m, 8H, N-CH$_2$-CH_2 (piper)], 1.42 [m, 4H, N-CH$_2$-CH$_2$-CH_2 (piper)], 1.37 [m, 4H, N-CH$_2$-CH$_2$-CH_2 (piper)]. ^{13}C NMR (100 MHz, $CDCl_3$, ppm, in Scheme 1 the numberings of carbons were given): δ 173.29 (s, COO^-), 157.65 (d, $^3J_{PC}$=10.0 Hz, C_1), 154.91 (s, C_f), 148.63 (s, C_5), 148.35 (s, C_c), 137.80 (s, C_3), 122.67 (s, C_a), 122.07 (s, C_2), 121.75 (s, C_4), 117.07 (s, C_d), 116.95 (s, C_b), 116.25 (s, C_e), 67.80 (d, $^2J_{PC}$=7.7 Hz, O-*C*H$_2$), 52.51 (d, $^2J_{PC}$=2.0 Hz, Py-*C*H$_2$-N), 47.06 (s, Py-CH$_2$-N-*C*H$_2$), 45.40 and 45.36 [s, N-*C*H$_2$ (piper)], 25.97 and 25.93 [(s, N-CH$_2$-*C*H$_2$ (piper)], 25.53 (s, N-CH$_2$-*C*H$_2$), 24.58 and 24.34 [(s, N-CH$_2$-CH$_2$-*C*H$_2$ (piper)].

Synthesis of 2-pyridyl(N/O)spirotetrapyrrolidino-PMOS (6b)

The work-up procedure was similar to that of compound **6a**, using **4b** (0.50 g, 0.86 mmol) and gentisic acid (0.13 g, 0.86 mmol). The reaction mixture was refluxed for over 45 h. After that, the solvent was evaporated under vacuo. A colourless powder of **6b** was crystallized from toluene. Yield: 0.46 g (73%). Anal. Calcd. for $P_3N_9O_5C_{32}H_{49}$, 732.31 g/mol: C, 52.49; H, 6.74; N, 17.21. Found: C, 51.99; H, 6.85; N, 16.96. FTIR (KBr, cm^{-1}): *v* 2967, 2870 (C-H aliph.), 2642 (N^+-H), 1571 (asymm.), 1374 (symm.) (COO^-), 1236 (asymm.), 1198 (symm.) (P=N). ^{1}H NMR (400 MHz, $CDCl_3$, ppm, in Scheme 1 the numberings of protons were given): δ 8.51 (d, H, $^3J_{HH}$=4.8 Hz, H_5), 7.71 (dd, H, $^3J_{HH}$=8.4 Hz, $^3J_{HH}$=7.2 Hz, H_3), 7.65 (d, H, $^3J_{HH}$=7.2 Hz, H_2), 7.58 (d, 1H, $^3J_{HH}$=3.2 Hz, H_b), 7.17 (dd, H, $^3J_{HH}$=7.2 Hz, $^3J_{HH}$=7.6 Hz, H_4), 6.87 (dd, 1H, $^3J_{HH}$=9.2 Hz, $^3J_{HH}$=3.2 Hz, H_d), 6.70 (d, 1H, $^3J_{HH}$=8.4 Hz, H_e), 4.46 (t, H, $^3J_{PH}$=11.6 Hz, $^2J_{HH}$=4.8 Hz, O-CH_2), 4.42 (t, H, $^3J_{PH}$=10.8 Hz, $^2J_{HH}$=4.8 Hz, O-CH_2), 4.22 (d, 2H, $^3J_{PH}$=8.8 Hz, Py-CH_2-N), 3.10 (m, H, Py-CH$_2$-N-CH_2), 3.20 [m, 8H, N-CH_2 (pyrr)], 3.15 [m, 8H, N-CH_2 (pyrr)], 1.92 (m, 2H, $^3J_{HH}$=5.2 Hz, $^3J_{HH}$=5.2 Hz, N-CH$_2$-CH_2), 1.79 [m, 8H, N-CH$_2$-CH_2 (pyrr)], 1.70 [m, 8H, N-CH$_2$-CH_2 (pyrr)]. ^{13}C NMR (100 MHz, $CDCl_3$, ppm, in Scheme 1 the numberings of carbons were given): δ 173.45 (s, COO^-), 158.03 (d, $^3J_{PC}$=9.3 Hz, C_1), 154.73 (s, C_f), 148.66 (s, C_5), 148.60 (s, C_c), 137.27 (s, C_3), 122.41 (s, C_a), 122.01 (s, C_2), 121.03 (s, C_4), 118.24 (s, C_d), 116.53 (s, C_b), 116.49 (s, C_e), 67.36 (d, $^2J_{PC}$=6.1 Hz, O-*C*H$_2$), 53.08 (s, Py-*C*H$_2$-N), 46.94 (s, Py-CH$_2$-N-*C*H$_2$), 46.43 and 46.29 [s, N-*C*H$_2$ (pyrr)], 26.35 [(d, $^3J_{PC}$=9.3 Hz, N-CH$_2$-*C*H$_2$ (pyrr)], 26.24 [(d, $^3J_{PC}$=9.2 Hz, N-CH$_2$-*C*H$_2$ (pyrr)], 26.19 (s, N-CH$_2$-*C*H$_2$).

Synthesis of 2-pyridyl(N/O)spirotetramorpholino-PMOS (6c)

The work-up procedure was similar to that of compound **6a**, using **4c** (0.50 g, 0.78 mmol) and gentisic acid (0.12 g, 0.78 mmol). The reaction mixture was refluxed for over 45 h. After that, the solvent was evaporated under vacuo. A colourless powder of **6c** was crystallized from toluene. Yield: 0.42 g (68%). M.P.: 139 °C. Anal. Calcd. for $P_3N_9O_9C_{32}H_{49}$, 796.29 g/mol: C, 48.27; H, 6.20; N, 15.83. Found: C, 48.80; H, 6.36; N, 15.87. FTIR (KBr, cm^{-1}): *v* 2955, 2843 (C-H aliph.), 2675 (N^+-H), 1595 (asymm.), 1367 (symm.) (COO^-), 1254 (asymm.), 1188 (symm.) (P=N). ^{1}H NMR (400 MHz, $CDCl_3$, ppm, in Scheme 1 the numberings of protons were given): δ 8.75 (d, H, $^3J_{HH}$=4.8 Hz, H_5), 7.81 (dd, H, $^3J_{HH}$=8.0 Hz, $^3J_{HH}$=7.2 Hz, H_3), 7.75 (d, H, $^3J_{HH}$=8.0 Hz, H_2), 7.41 (d, 1H, $^3J_{HH}$=3.2 Hz, H_b), 7.32 (dd, H, $^3J_{HH}$=7.2 Hz, $^3J_{HH}$=6.8 Hz, H_4), 6.98 (dd, 1H, $^3J_{HH}$=8.4 Hz, $^3J_{HH}$=2.8 Hz, H_d), 6.83 (d, 1H, $^3J_{HH}$=8.8 Hz, H_e), 4.41 (t, H, $^3J_{PH}$=10.6 Hz, $^2J_{HH}$=5.8 Hz, O-CH_2), 4.38 (t, H, $^3J_{PH}$=10.4 Hz, $^2J_{HH}$=6.0 Hz, O-CH_2), 4.17 (d, 2H, $^3J_{PH}$=8.8 Hz, Py-CH_2-N), 3.64 [m, 8H, O-CH_2 (morp)], 3.56 [m, 8H, O-CH_2 (morp)], 3.12 (m,

H, Py-CH_2-N-CH_2), 3.08 [m, 16H, N-CH_2 (morp)], 1.95 (m, 2H, $^3J_{HH}$=4.8 Hz, $^3J_{HH}$=5.6 Hz, N-CH_2-CH_2). ^{13}C NMR (100 MHz, $CDCl_3$, ppm, in Scheme 1 the numberings of carbons were given): δ 172.90 (s, COO^-), 157.66 (d, $^3J_{PC}$=11.6 Hz, C_1), 155.64 (s, C_f), 148.79 (s, C_5), 147.58 (s, C_c), 138.69 (s, C_3), 123.56 (s, C_a), 122.97 (s, C_2), 121.96 (s, C_4), 118.10 (s, C_d), 114.69 (s, C_b), 113.26 (s, C_e), 67.12 [(s, O-*C*H_2 (morp)], 67.09 [(s, O-*C*H_2 (morp)], 66.92 (d, $^2J_{PC}$=7.6 Hz, O-*C*H_2), 52.21 (s, Py-*C*H_2-N), 47.48 (s, Py-CH_2-N-*C*H_2), 44.66 and 44.60 [s, N-*C*H_2 (morp)], 26.66 (s, N-CH_2-*C*H_2).

Synthesis of 2-pyridyl(N/O)spirotetraDASD-PMOS (6d)

The work-up procedure was similar to that of compound **6a**, using **4d** (0.50 g, 0.58 mmol) and gentisic acid (0.09 g, 0.58 mmol). The reaction mixture was refluxed for over 45 h. After that, the solvent was evaporated under vacuo. A colourless powder of **6d** was crystallized from toluene. Yield: 0.46 g (77%). M.P.: 119 °C. Anal. Calcd. for $P_3N_9O_{13}C_{44}H_{65}\cdot C_7H_8$, 1112.42 g/mol: C, 55.07; H, 6.61; N, 11.33. Found: C, 54.71; H, 6.35; N, 10.99. FTIR (KBr, cm^{-1}): *v* 2956, 2852 (C-H aliph.), 2668 (N^+-H), 1593 (asymm.), 1379 (symm.) (COO^-), 1258 (asymm.), 1196 (symm.) (P=N). ^{1}H NMR (400 MHz, $CDCl_3$, ppm, in Scheme 1 the numberings of protons were given): δ 8.57 (d, H, $^3J_{HH}$=4.4 Hz, H_5), 7.72 (dd, H, $^3J_{HH}$=7.6 Hz, $^3J_{HH}$=7.6 Hz, H_3), 7.66 (d, H, $^3J_{HH}$=7.6 Hz, H_2), 7.42 (d, 1H, $^3J_{HH}$=3.2 Hz, H_b), 7.14 (dd, H, $^3J_{HH}$=7.6 Hz, $^3J_{HH}$=7.2 Hz, H_4), 6.93 (dd, 1H, $^3J_{HH}$=8.2 Hz, $^3J_{HH}$=3.2 Hz, H_d), 6.76 (d, 1H, $^3J_{HH}$=8.8 Hz, H_e), 4.45 (t, H, $^3J_{PH}$=10.4 Hz, $^2J_{HH}$=4.8 Hz, O-CH_2), 4.41 (t, H, $^3J_{PH}$=10.0 Hz, $^2J_{HH}$=4.8 Hz, O-CH_2), 4.21 (d, 2H, $^3J_{PH}$=9.2 Hz, Py-CH_2-N), 3.92 [s, 8H, O-CH_2 (DASD)], 3.83 [s, 8H, O-CH_2 (DASD)], 3.16 [m, 16H, N-CH_2 (DASD)], 3.20 (m, H, Py-CH_2-N-CH_2), 1.90 (m, 2H, $^3J_{HH}$=4.8 Hz, $^3J_{HH}$=5.2 Hz, N-CH_2-CH_2), 1.66 [m, 8H, N-CH_2-CH_2 (DASD)], 1.55 [m, 8H, N-CH_2-CH_2 (DASD)]. ^{13}C NMR (100 MHz, $CDCl_3$, ppm, in Scheme 1 the numberings of carbons were given): δ 173.07 (s, COO^-), 157.65 (d, $^3J_{PC}$=10.7 Hz, C_1), 155.22 (s, C_f), 148.51 (s, C_5), 148.10 (s, C_c), 137.89 (s, C_3), 122.63 (s, C_a), 122.43 (s, C_2), 122.35 (s, C_4), 118.67 (s, C_d), 117.45 (s, C_b), 115.53 (s, C_e), 107.33 and 107.10 [s, O-*C*-O (DASD)], 67.33 (d, $^2J_{PC}$=6.8 Hz, O-*C*H_2), 52.48 (s, Py-*C*H_2-N), 47.00 (s, Py-CH_2-N-*C*H_2), 64.23 and 64.14 [s, O-*C*H_2 (DASD)], 42.72 [s, N-*C*H_2 (DASD)], 35.35 [s, N-CH_2-*C*H_2 (DASD)], 26.24 (d, $^3J_{PC}$=3.8 Hz, N-CH_2-*C*H_2).

Synthesis of 2-pyridyl(N/N)spirotetrapiperidino-PMOS (7a)

The work-up procedure was similar to that of compound **6a**, using **5a** (0.50 g, 0.77 mmol) and gentisic acid (0.12 g, 0.77 mmol). The reaction mixture was refluxed for over 45 h. After that, the solvent was evaporated under vacuo. A colourless powder of **7a** was crystallized from toluene. Yield: 0.36 g (58%). Anal. Calcd. for $P_3N_{10}O_4C_{37}H_{60}$, 801.40 g/mol: C, 55.45; H, 7.55; N, 17.48. Found: C, 55.08; H, 7.69; N, 17.09. FTIR (KBr, cm^{-1}): *v* 3198 (O-H), 2925, 2850 (C-H aliph.), 2632 (N^+-H), 1591 (asymm.), 1372 (symm.) (COO^-), 1244 (asymm.), 1159 (symm.) (P=N). ^{1}H NMR (400 MHz, $CDCl_3$, ppm, in Scheme 1 the numberings of protons were given): δ 8.58 (d, H, $^3J_{HH}$=4.8 Hz, H_5), 8.45 (b, 2H, Ar-O*H*), 7.78 (dd, H, $^3J_{HH}$=8.0 Hz, $^3J_{HH}$=7.6 Hz, H_3), 7.70 (d, H, $^3J_{HH}$=7.6 Hz, H_2), 7.52 (d, 1H, $^3J_{HH}$=2.8 Hz, H_b), 7.15 (dd, H, $^3J_{HH}$=8.0 Hz, $^3J_{HH}$=7.6 Hz, H_4), 6.98 (dd, 1H, $^3J_{HH}$=8.8 Hz, $^3J_{HH}$=3.0 Hz, H_d), 6.75 (d, 1H, $^3J_{HH}$=8.8 Hz, H_e), 4.30 (d, 2H, $^3J_{PH}$=9.2 Hz, Py-CH_2-N), 3.31 (m, 2H, CH_3-N-CH_2), 3.03 (m, 2H, Py-CH_2-N-CH_2), 3.10 [m, 8H, N-CH_2 (piper)], 2.97 [m, 8H, N-CH_2 (piper)], 2.71 (d, 3H, $^3J_{PH}$=12.0 Hz, N-CH_3), 1.88 (m, $^3J_{HH}$=5.2 Hz, $^3J_{HH}$=5.2 Hz, 2H, N-CH_2-CH_2), 1.51 [m, 16H, N-CH_2-CH_2 (piper)], 1.35 [m, 4H, N-CH_2-CH_2-CH_2 (piper)], 1.33 [m, 4H, N-CH_2-CH_2-CH_2 (piper)]. ^{13}C NMR (100 MHz, $CDCl_3$, ppm, in Scheme 1 the numberings of carbons were given): δ 173.47 (s, COO^-), 157.85 (d, $^3J_{PC}$=9.2 Hz, C_1), 155.31 (s, C_f), 149.14 (s, C_5), 148.53 (s, C_c), 138.34 (s, C_3), 123.26 (s, C_a), 123.12 (s, C_2), 122.24 (s, C_4), 116.19 (s, C_d), 117.63 (s, C_b), 115.19 (s, C_e), 51.53 (m, Py-*C*H_2-N), 50.61 (s, Py-CH_2-N-*C*H_2), 47.28 (s, *C*H_3-N-CH_2), 45.91 and 45.75 [s, N-*C*H_2 (piper)], 35.69 (m, N-CH_3), 25.30 (s, N-CH_2-*C*H_2), 26.31 and 26.17 [(s, N-CH_2-*C*H_2 (piper)], 24.73 and 24.55 [(s, N-CH_2-CH_2-*C*H_2 (piper)].

Evaluation of in vitro antimicrobial activity

In the present study, the antimicrobial effects of the free phosphazene bases (**4a-4d** and **5a-5d**) and PMOSs (**6a-6d** and **7a**) were assessed in order to discover the potential antimicrobial agents against the selected bacteria and yeast strains. The free phosphazene bases (**4a-4d** and **5a-5d**) and PMOSs were tested comparatively for their *in vitro* antibacterial activities against five G(+) {*Enterococcus faecalis* ATCC 29212, *Enterococcus hirae* ATCC 10541, *Staphylococcus aureus* ATCC 25923, *Bacillus subtilis* ATCC 6633, *Bacillus cereus*

NRRL B-3711}, and three G(-) {*Proteus vulgaris* ATCC 8427*, Salmonella typhimurium* ATCC 14028*, Klebsiella pneumaniae* ATCC 13883} bacteria, and also for their antifungal activities against three fungi {*Candida albicans* ATCC 10231*, Candida krusei* ATCC 6258*, Candida tropicalis* Y-12968} using the agar-well diffusion method.[42] Microorganisms were acquired from the collections of Gazi University Molecular Biology Culture Collection, Turkey. For positive control, ampicillin (10 μg/mL) and chloramphenicol (30 μg/mL) were selected as the reference antibacterial agents, and ketoconazole (50 μg/mL) was used as reference antifungal agent. The susceptibility testing was performed using the BACTEC MGIT 960 (Becton Diskinson, Sparks, MD) systems. Dimethyl sulfoxide (DMSO) was used as the negative control since it was used as the solvent for all the compounds. G(-) and G(+) bacteria were grown on nutrient broth agar plates and incubated at 37 °C for 24 h. Whilst, the yeast strains were grown in Sabouraud dextrose agar (SDA) medium and incubated at 30 °C for 48 h. After incubation, bacterial suspensions were adjusted to a turbidity of 0.5 McFarland. SDA (for fungal strains) and Mueller Hinton agar (MHA) (for bacterial strains) were mixed with 1% culture suspension and poured into plates. A suspension of the tested microorganism was spread over the surface of agar plates (SDA and MHA). The testing compounds (2000 μM) were added into the wells. The diameter of the inhibition zone was measured in millimeters.

The minimum inhibitory concentration (MIC), minimum bactericidal concentration (MBC) and minimum fungicidal concentration (MFC) values of the active compounds were also determined with the broth microdilution method.[43] A preculture of bacteria was grown in Lysogeny broth (LB) overnight at 37 °C. The bacteria were treated with various concentrations of the compounds.

Determination of the DNA and compound interactions

To evaluate the interactions between the compound and DNA, the agarose gel electrophoresis technique was performed using plasmid DNA.[44] The stock solutions of the free phosphazene bases (**4a-4d** and **5a-5d**) and PMOSs (**6a-6d** and **7a**) in DMSO were prepared and used within 1 h. Then, aliquots of decreasing concentrations of the compounds ranging from 2000 to 250 μM were incubated with supercoiled plasmid DNA in an incubator at 37 °C for 24 h in the dark. The compound/DNA mixtures were loaded onto the agarose gel with a loading buffer (0.1% bromophenol blue, 0.1% xylene cyanol). The agarose gel electrophoresis was made under TAE buffer (0.05 M Tris base, 0.05 M glacial acetic acid and 1 mM EDTA, pH = 8.0) for 3 h at 60 V. After that, the gel was stained with ethidium bromide (0.5 μg/mL), visualized under UV light using a transilluminator (BioDoc Analyzer, Biometra) and the image was photographed with a video camera. Each experiment was repeated for three times and the mean values were given.

HindIII and BamHI digestions of the compound-plasmid DNA mixture

The affinity evaluation between the prepared compounds (**4a-7a** and **4d-6d**) and guanine-guanine (G/G) and/or adenine-adenine (A/A) regions was investigated through restriction endonuclease analysis.[45] Compound/DNA mixtures were incubated for 24 h, and then restricted with *Hind*III and *BamH*I enzymes at 37 °C. The restricted DNA was run in agarose gel electrophoresis for 1 h at 70 V in TAE buffer.[44] The gel was stained with ethidium bromide (0.5 μg/mL), and then the gel was viewed with a transilluminator, and the image was photographed with a video-camera and saved as a TIFF file.

*Bam*HI enzyme binds at the sequence 5'-G/GATCC-3' and since pBR322 plasmid DNA contains a single sequence of that, cleaves this sequence. *Bam*HI then converts supercoiled Form I and open circular Form II to linear form of linear DNA (Form III). *Hind*III recognizes the sequence 5'-A/AGCTT-3' and cleaves this sequence. As a result, *Hind*III converts Form I and Form II to Form III similarly to *Bam*HI.

Determination of the cytotoxic activity with WST-1 method

The cell viability was examined using WST-1 assay.[46] Normal L929 fibroblast cells (healthy cell group, 5×10^3 cells per well) and MDA-MB-231 (5×10^3 cells per well) breast cancer cells were placed in flasks containing Dulbecco's Modified Eagle's medium (DMEM) and Roswell Park Memorial Institute (RPMI) 1640, respectively, with L-glutamine, 10% FCS, and 1% antibiotic. They were kept in a CO_2 incubator conditioned with 5% CO_2 at 37 °C for 48 h until the cells attached to the bottom of the plate, then the cell culture medium was replaced with fresh medium and different concentrations (100-12.5 μg/mL) of the compounds were placed into the wells. The cell culture medium was removed

and the cells were treated with trypsin-EDTA (0.5 mL per flask) for harvesting cells, Afterwards, the cells were transferred into 15 mL Eppendorf tubes and centrifuged at 2.500 rpm for 2 min. The cells were used after removing the supernatant in the cytotoxic activity studies. Doxorubicin was used at various concentrations as positive control. The plates containing DMEM with L-glutamine, 10% FCS, and 1% antibiotic and RPMI with L-glutamine, 10% FCS, and 1% antibiotic were incubated at 37 °C in an incubator for 24 h. Following 24 h incubation under the same conditions, WST-1 (a water-soluble tetrazolium salt) reagent (5 µL) was added into each well. Upon incubation for an additional 4 h, the plates were immediately read in an Elisa Microplate Reader (BioTek, USA) at 440 nm wavelength and the percentage of cell viability of each group was calculated according to the definition of the control cell viability as 100%.

Determination of the antituberculosis activity against Mycobacterium tuberculosis

The agar proportion method was performed using Middlebrook 7H10 agar. This is a reference method for drug susceptibility testing of *Mycobacterium tuberculosis* according to CLSI recommendations.[47,48] The final concentration of each compound in the medium was firstly adjusted to 5, 10, 20, 40 and 80 µg/mL, respectively. The final concentrations were changed for the compounds displaying antituberculosis activity to *M. tuberculosis* H37Rv strain, to detect minimal inhibition concentration (MIC) of compounds. Middlebrook 7H10 medium was prepared and autoclaved at 121°C for 10 minutes. When cooled to 55 °C, Middlebrook 7H10 medium was mixed with Middlebrook OADC Enrichment and dissolved compounds, before pouring into the Petri dish bottom divided into four partitions. Quality controls of media were done.

Results and Discussion

Syntheses and characterizations

The syntheses of PMOSs (**6a-6d** and **7a**) were achieved by the reactions of the corresponding free cyclotriphosphazene bases (**4a-4d** and **5a**) with gentisic acid in dry THF (Scheme 1). These types of the PMOS are the first examples of pyridyl substituted phosphazenium salts synthesized from the reactions of the cyclotriphosphazene free bases and bulky gentisic acid. The reaction yields of the PMOS were calculated in the range of (58–77)%. In addition, all of the PMOSs (**6a-6d** and **7a**) were slightly soluble in hot water, however, fairly soluble in the common organic apolar/polar solvents. The salts **6b** and **7a** were the waxy solids, whereas **6a, 6c** and **6d** were solid at ambient temperature. The melting points (mp) of **6a, 6c** and **6d** are 105, 139 and 119 °C, respectively. The crystallization of the PMOS for X-ray diffraction analysis was not easy, so only the suitable crystals of **6c** were obtained. The X-ray crystallographic results display that **6c** was protonated with the N atom of the cyclotriphosphazene ring near to the N/O spiro ring. In contrast, it was observed in the literature that the protonation in 4-fluorobenzylspiro(N/O)cyclotriphosphazenes took place on the nitrogen atom of the phosphazene ring which is non-adjacent to the N/O spiro ring.[28,29] The data obtained from the NMR spectra of the other salts show that all the PMOSs are likely to be protonated in the nitrogen atom of the phosphazene ring.

The proposed structures of the cyclotriphosphazene (**5a**) and PMOSs (**6a–6d** and **7a**) were evaluated using the ESI-MS (for **5a,** in Supplementary Data, Fig. S1), FTIR, ^{1}H, $^{13}C\{^{1}H\}$ and $^{31}P\{^{1}H\}$ NMR data.

NMR and IR spectroscopy

The $^{31}P\{^{1}H\}$ NMR results were presented in Table 2 together with the corresponding bases (**4a–4d** and **5a**) and their gentisic acid salts (**6a–6d** and **7a**). The ^{31}P NMR data of the free bases are taken from the literature for comparison purposes. The spin systems of the PMOS were determined as AX_2 (**6a, 6d** and **7a**) and AB_2 (**6b** and **6c**). Since the proton can exchange between the N atoms of the cyclotriphosphazene ring in the $CDCl_3$ solution at the ambient temperature. Otherwise, as expected the spin systems of the PMOS ought to be as ABX or AMX. The ^{31}P NMR spectra of **6c** were also recorded at low temperatures, −28 °C, −20 °C, −10 °C, +10 °C and +25 °C, to confirm that the proton was displaced between the N atoms of the cyclotriphosphazene ring (Fig. 1). The spectra of **6c** show that the spin system does not change even at −28 °C in the $CDCl_3$ solution. It is deduced from this finding that the H^+ ion displaces between the nitrogen atoms even at low temperatures.

On the other hand, in all the PMOSs, the P1 phosphorus atoms ought to be chiral centres, and they are expected to form a racemic mixture (R and S). Actually, the solid-state structure of **6c** was proved crystallographically (see X-ray part 3.4). The space

Table 2 — ^{31}P {^{1}H} NMR parameters of 2-pyridylspirocyclotriphosphazenes and their PMOSs[a]

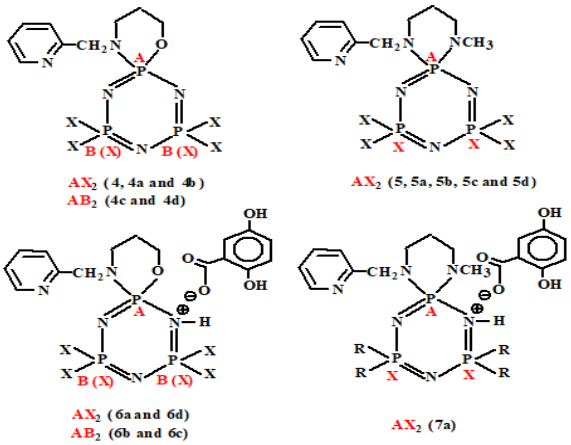

Comp.	Spin Systems	$P_{NO(spiro)}$	$P_{NN(spiro)}$	P_{NN}	P_{Cl2}	$^{2}J_{PP}$ (Hz)	$^{2}J_{PP}/\Delta\nu$
*4	AX_2	8.92 (t)	-	-	23.39 (d)	$^{2}J_{AX}$ 38.9	-
*5	AX_2	-	11.66 (t)	-	22.02 (d)	$^{2}J_{AX}$ 38.9	-
*4a	AX_2	20.20 (t)	-	22.22 (d)	-	$^{2}J_{AX}$ 43.7	-
*4b	AX_2	21.14 (t)	-	18.89 (d)	-	$^{2}J_{AX}$ 43.7	-
*4c	AB_2	20.05 (t)	-	21.44 (d)	-	$^{2}J_{AB}$ 46.2	0.14
*4d	AB_2	19.70 (t)	-	21.30 (d)	-	$^{2}J_{AB}$ 48.6	0.13
5a	AX_2	-	23.39 (t)	21.13 (d)	-	$^{2}J_{AX}$ 38.9	-
*5b	AX_2	-	23.79 (t)	17.39 (d)	-	$^{2}J_{AX}$ 38.9	-
*5c	AX_2	-	23.25 (t)	20.14 (d)	-	$^{2}J_{AX}$ 38.9	-
*5d	AX_2		23.00 (t)	20.33 (d)	-	$^{2}J_{AX}$ 36.4	-
6a	AX_2	13.70 (t)	-	17.82 (d)	-	$^{2}J_{AX}$ 41.3	-
6b	AB_2	15.21 (t)	-	14.52 (d)	-	$^{2}J_{AB}$ 38.9	0.23
6c	AB_2	19.85 (t)	-	21.03 (d)	-	$^{2}J_{AB}$ 43.7	0.15
6d	AX_2	16.81 (t)	-	19.29 (d)	-	$^{2}J_{AX}$ 43.7	-
7a	AX_2	-	13.24 (t)	15.98 (d)	-	$^{2}J_{AX}$ 31.6	-

[a]242.93 MHz ^{31}P {^{1}H} NMR measurements in $CDCl_3$ solutions at 298 K, and the chemical shifts referenced to external H_3PO_4.
*^{31}P {^{1}H} NMR values of these compunds were taken from the literature references 35 and 36.

group is found to be as *P-1,* which is amongst the Sohncke space groups.[49,50] This compound in the solid state may be locked-conformation, and so it is chiral as it does not convert to its mirror image.[49] Taking into account of the crystallographic check CIF report, **6c** had one chiral P center, and the absolute configuration of P1 center is found to be as R, exhibiting that there was solely single enantiomer in the unit cell in the solid state. But, since the proton is displaced between the nitrogen atoms in solution, the chirality disappears. It is noteworthy that this finding is observed for the first time in phosphazenium salts.

The coupling constants, $^{2}J_{PP}$, of the PMOSs (**6a–6d** and **7a**) (31.6–43.7 Hz) are slightly smaller than those of the corresponding phosphazene bases (**4a–4d** and **5a**) (38.9–48.6 Hz). They are a good agreement with the literature values of the phosphazenium salts.[28-31] The δ P (spiro) (13.24–19.85 ppm) and δ P_{NN} shifts (14.52–21.03 ppm) are smaller than those of the free phosphazene bases; the δ P (spiro) (19.70–23.39 ppm) and δ P_{NN} shifts (18.89–22.22 ppm). As an example, the $^{31}P\{^{1}H\}$ NMR spectra of **6a** and **6d** were depicted in Fig. 2. Consequently, all these findings are evidence of the protonations of the free bases.

The signals of the carbons and protons of the free base (**5a**) and PMOSs (**6a–6d** and **7a**) were assigned from the ^{13}C and ^{1}H spectra. The ^{13}C and ^{1}H NMR spectra of the PMOS **6a** were given in Supplementary Data, Figs S2 and S3. The obtained ^{13}C NMR data were given in "Experimental Part". The O-$\underline{C}H_2$ carbons of the PMOS were observed in the range of 66.92–67.80 ppm, and the average value of $^{2}J_{\underline{P}O\underline{C}}$ is 7.1 Hz. The average $^{3}J_{\underline{P}NC\underline{C}}$ value for the N-CH_2-$\underline{C}H_{2(pyrr)}$ carbons is 9.3 Hz. In addition, the carbon peaks of the

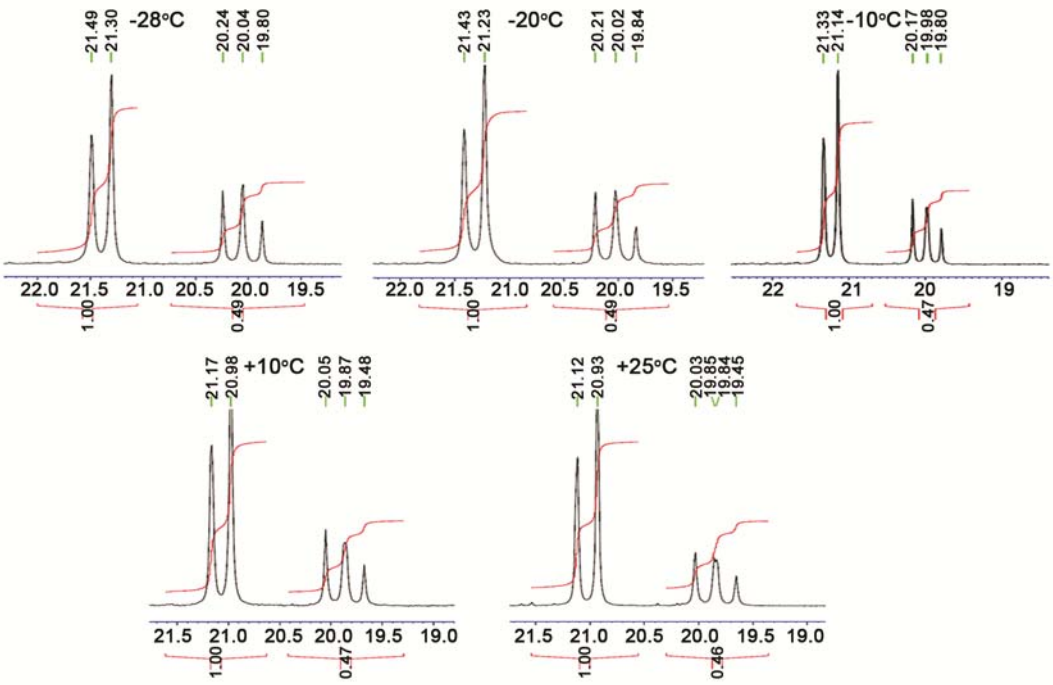

Fig. 1 — ^{31}P NMR spectra of **6c** at varying temperatures (-28 °C, -20 °C, -10 °C, +10 °C and +25 °C)

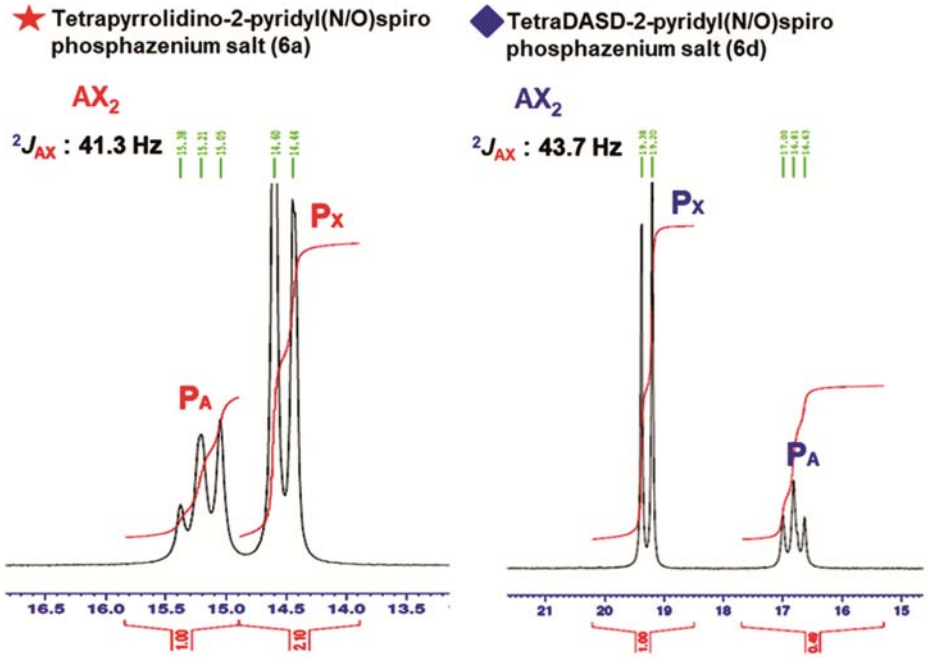

Fig. 2 — ^{31}P {^{1}H} NMR spectra of the compounds **6a** and **6d**

pyridyl ring (C_1-C_5) were interpreted from the ^{13}C spectra of the compounds. In piperidine (**6a** and **7a**) and pyrrolidine (**6b**) substituted PMOSs, the $^{3}J_{\underline{PNCC}}$ values of C_1 carbons of the pyridyl rings are smaller than those of the corresponding free phosphazene bases except of morpholine (**6c**) and DASD (**6d**) substituted ones. On the other hand, the *geminal* substituents of all the compounds exhibit two small separated peaks for N-$\underline{C}H_2$ (except **6d**), N-CH_2-$\underline{C}H_2$ (except **6d**), N-CH_2-CH_2-$\underline{C}H_2$ (for **5a, 6a** and **7a**), O-$\underline{C}H_2$ (for **6c** and **6d**) and O-$\underline{C}$-O groups (for **6d**), since two *geminal* groups are not equivalent to each other. The O-$\underline{C}$-O and C-O-$\underline{C}H_2$ carbon signals of **6d** were observed at 107.33; 107.10, and 64.23; 64.14 ppm,

respectively, as four separate singlets. In addition, the second order effect at ca. 26 ppm in the ^{13}C spectrum of **6b** was observed. The average $^{3}J_{\underline{P}NC\underline{C}}$ value was calculated as 8.9 Hz taking the external transitions of the triplets (Supplementary Data, Fig. S4). The similar observations were reported in the literature for some pyrrolidino phosphazene derivatives. The obtained $^{3}J_{\underline{P}NC\underline{C}}$ value is consistent with the literature data.[35,36] The interpretations of the δ-shifts of *C*OO$^-$ and C_a-C_f carbons of the gentisic acid ions were also made in the PMOS (Fig. 1), and the results were proved to be in compliance with the literature data.[28,29]

The obtained ^{1}H NMR data were presented in "Experimental Part". The integral ratio in ^{1}H spectrum of **5a** shows that four Cl atoms were replaced by piperidine. The δ_H-shifts of all the PMOSs have almost the same δ_H values with the corresponding free bases.[35,36] Furthermore, in the PMOS, the $^{3}J_{\underline{P}NC\underline{H}}$ values of Py-C$\underline{H}_2$-N protons are larger than those of the corresponding free phosphazene bases[35,36]. The N-C$\underline{H}_3$ protons of the free base (**5a**) and PMOS (**7a**) were observed in 2.57 ppm and 2.71 ppm, respectively. The large $^{3}J_{\underline{P}NC\underline{H}}$ values were calculated as 13.2 Hz and 12.0 Hz from the doublets of the spectra of **5a** and **7a**, respectively. Furthermore, the δ-shifts and coupling constants of H_b, H_d and H_e protons of the gentisic acid ions were evaluated (Fig. 1), and the findings are in agreement with the literature data.[28,29]

The characteristic FTIR bands of the free base (**5a**) and PMOSs (**6a–6d** and **7a**) were given in "Experimental Part". The sharp asymmetric and symmetric vibrations are observed between 1258–1240 cm^{-1} and 1198-1151 cm^{-1}, referred to the P=N bonds of the P_3N_3 rings.[51,52] The $\nu_{(N^+\text{-}H)}$ stretching bands of the PMOSs (**6a–6d** and **7a**) were observed in the range of 2675–2632 cm^{-1}. Two strong characteristic bands in the ranges of 1595–1571 cm^{-1} and 1379–1367 cm^{-1}, which are determined to the asymmetric and symmetric vibrations of $\nu_{(COO^-)}$ bonds, respectively prove the PMOS formation.[28,29] Besides, the only 2-pyridyl(N/N)spirotetrapiperidino-PMOSs (**6a** and **7a**) exhibit the $\nu_{O\text{-}H}$ (ca. 3200 cm^{-1}) absorption frequencies.

The microanalytical, IR, NMR (^{1}H, ^{13}C, and ^{31}P) and X-ray structural data (for **4a** and **6c**) exhibit that the molecular structures of the compounds are consistent with the proposed structures in Scheme 1.

Thermal studies

In the last decades, the thermal properties of the cyclotriphosphazenes and their phosphazenium salts (PMOS) were investigated using DSC and TG/DTA techniques.[29-31] Generally, these methods are significantly helpful for the material science to understand the thermal stabilities and flame-retardant properties of the inorganic, organic and polymeric materials.[53,54] The TG thermograms of the PMOSs (**6a–6d** and **7a**) which are measured using same experimental conditions are shown in Supplementary Data, Fig. S5. Thermoanalytical data of the PMOS were also listed in Table 3.

Taking into account of the TG graphs, there are some diversity in the thermal properties of the PMOS. The quantity of the total mass loss in the PMOS is almost the same, and the non-volatile inorganic phosphorus and nitrogen residues are in the range of 7.87–11.92 weight%. In addition, all of the PMOS have somewhat different thermal decomposition routes, and consist of two (**6c**), three (**6d** and **7a**) and four (**6a** and **6b**) steps (Table 3). The PMOSs (except **6c**) incorporate toluene molecules with respect to the thermal analysis results. In the first step, toluene molecules are separated from the structures in the PMOSs (except **6a**). After the separation of the toluene molecules, gentisic acid anions leave the structure (except **6a**). Later, the pyridyl pendant armed, which forms the spiro ring and secondary amine precursors decompose and leave from the structure. Thermoanalytical data of **6a, 6b** and **7a** display that these salts decompose at lower temperatures than the other PMOSs (**6c** and **6d**). Thermal stability (788 °C) of **7a,** which has N/N spiro ring is lower than those of the others.

X-Ray structures of 4a and 6c

The crystal structure determinations of **4a** and **6c** were made using their X-ray crystallographic data. The molecular structures of these compounds along with the atom-numbering schemes were illustrated in Figs 3 and 4, respectively. The characteristic bond lengths and angles were presented in Table 4. The conformations of the cyclotriphosphazene rings of **4a** and **6c** were illustrated by the torsion angles of the P3N3 ring bonds, showing that both of them were not pseudo-centrosymmetric (Supplementary Data, Fig. S6). In **4a** and **6c**, the N/O donor type ligand was bonded to the P atoms in spiro fashion, and the six-membered N_3P_3 phosphazene rings (P1/N1/P2/N2/P3/N3) are found to be almost planar

Table 3 — Thermoanalytical data of the PMOSs

Comp.	Melting points (°C)	Stages	Temperature ranges (°C)	$DTG_{(max)}$ (°C)	Mass loss (Theo.) Δm %	Mass loss (Obs.) Δm %	Leaving groups	Mass of residues (Obs.) Δm % (residual group)
6a	105	1	68–245	189	17.38	17.12	Gentisic acid anion	10.12
		2	245–349	275	19.32	18.65	C_7H_8+Py	(N_2P_2)
		3	349–544	442	17.51	18.27	CH_2-N-$(CH_2)_3$+Piper.	
		4	544–1150	813	35.69	35.84	3Piper.+OP-NH	
6b	a waxy solid	1	65–180	122	11.17	12.01	C_7H_8	7.87
		2	180–368	267	25.60	25.03	Gentisic acid anion+$O(CH_2)_3$	(NP_2)
		3	368–573	439	12.99	12.54	Py-CH_2-NH	
		4	573–1150	870	41.15	42.50	4Pyrr.+NP-NH	
6c	139	1	123–530	277	45.35	45.38	Gentisic acid anion+$O(CH_2)_2$+ Py-CH_2-N-$(CH_2)_3$-O	10.30 (NP_2)
		2	530–1150	794	45.23	44.32	3Morp.+N-$(CH_2)_2$+NP-NH	
6d	119	1	92–224	189	7.64	7.87	C_7H_8	9.93
		2	224–554	265	46.26	49.44	Gentisic acid anion+ 4[$O(CH_2)_2O$]+ Py-CH_2-N-$(CH_2)_3$-O	(N_2P_2)
		3	554–1150	954	31.07	32.76	4[C-$(CH_2)_4$-N]+P-NH	
7a	a waxy solid	1	59–235	213	10.30	10.51	C_7H_8	11.92
		2	235–549	304	50.17	49.73	Gentisic acid anion+3Piper.+ CH_2-N-CH_3	(N_3P_2)
		3	549–1150	788	27.89	27.84	Piper.+Py-CH_2-NP-$(CH_2)_2$	

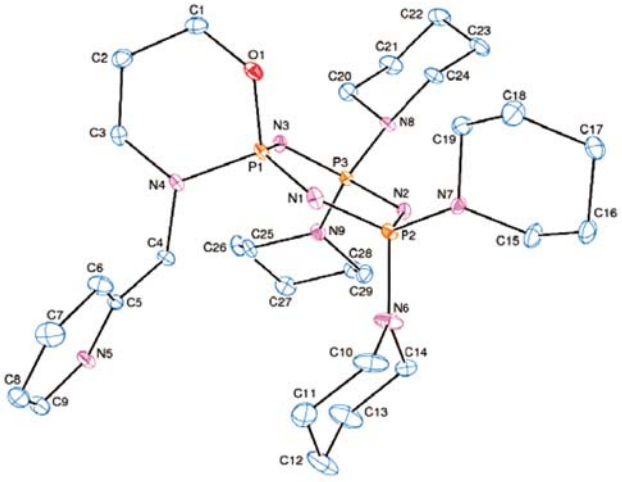

Fig. 3 — An ORTEP-3[56,57] drawing of **4a** with the atom-numbering scheme. Displacement ellipsoids are drawn at the 30% probability level

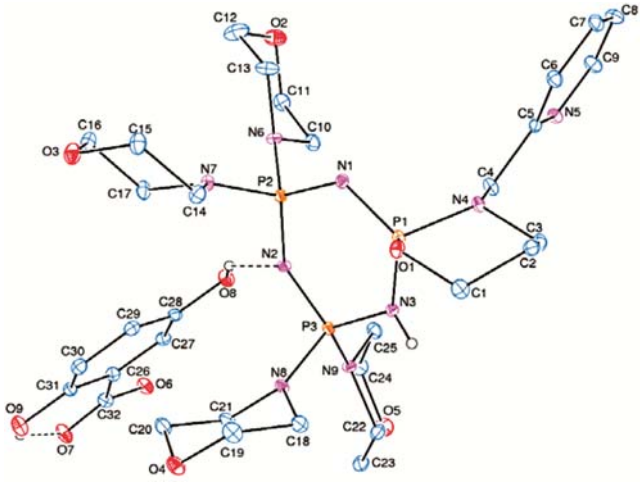

Fig. 4 — An ORTEP-3[56,57] drawing of **6c** with the atom-numbering scheme. Displacement ellipsoids are drawn at the 30% probability level

[Supplementary Data, Fig. S7a; the puckering parameters, Q_T,[55] 0.153(2) Å, φ_2= −161.5(9)°, θ_2= 62.5(9)° for **4a** and Supplementary Data, Fig. S8(a); Q_T= 0.200(2) Å, φ_2= 29.1(9)°, θ_2= 138.4(5)° for **6c**]. In addition, the six-membered spiro rings (P1/O1/C1/C2/C3/N4) of **4a** and **6c**, have chair [Fig. S7b; Q_T= 0.982(8) Å, φ_2= – 25.9(5)°, θ_2= 118.8(2)°] and twisted [Supplementary Data, Fig. S8(b); Q_T = 1.003(8) Å, φ_2= – 28.5(5)°, θ_2= 123.3(2)°] conformations, respectively.

The average endocyclic P—N bond lengths of **4a** and **6c** are incidentally found to be like the same,

1.593(3) Å (Table 4). The average exocyclic P–N bond lengths of **4a** and **6c** are also calculated as 1.656(3) Å and 1.654(3) Å, respectively. They are longer than those of the average endocyclic P–N bond lengths. The average N–P–N bond angle of the free phosphazene base **4a** is calculated as 117.25(14)°, which is slightly larger than that of the salt **6c** [115.96(15)°]. Whilst, the average P–N–P bond angles of **4a** and **6c** are found to be as almost the same, and they are 122.01(7)° and 122.46(17)°, respectively. The variations of the P–N–P and N–P–N bond angles of these compounds are very small as compared to the other aminophosphazenes and phosphazenium salts.[28-31,36] (Table 4).

Furthermore, the hydrogen bond geometries of the PMOS **6c** were listed in Supplementary Data, Table S1, and the packing diagram was also illustrated in Supplementary Data, Fig. S9. The intramolecular N—H···O hydrogen bond connects the gentisic acid ion to the cyclotriphosphazene ring (Fig. 4). The crystallographic data of the compounds **4a** and **6c** were stored with the Cambridge Crystallographic Data Centre, CCDC Nos 1853961 (for compound **4a**) and 1853962 (for compound **6c**).

Antimicrobial activities

The free phosphazene bases (**4a–4d** and **5a–5d**) and PMOSs (**6a–6d** and **7a**) were screened against the five G (+) (Table 5) and three G (−) (Table 6) bacteria and three fungi (Table 7) for their antimicrobial activities by the agar well diffusion method.[58] The antibacterial activities against *B. subtilis* G (+) of the compounds **5a** and **7a** are higher than those of ampisilin and chloramphenicol. However, the antibacterial activities against *B. subtilis* of **4a**

Table 4 — The Selected bond lengths (Å) and angles (deg) for **4a** and **6c**

	4a	**6c**		**4a**	**6c**
P1–N1	1.571(3)	1.572(3)	N1–P1–N3	118.07(15)	116.66(16)
P1–N3	1.591(3)	1.590(3)	N1–P2–N2	116.95(14)	115.72(15)
P2–N1	1.606(3)	1.589(3)	N2–P3–N3	116.73(14)	115.51(15)
P2–N2	1.591(3)	1.610(3)	N3–P1–N4	111.42(14)	110.02(14)
P3–N3	1.599(3)	1.578(3)	P1–N1–P2	122.40(17)	123.93(18)
P3–N2	1.597(3)	1.617(3)	P3–N2–P2	121.64(17)	120.55(17)
P2–N6	1.645(3)	1.661(3)	P1–N3–P3	122.01(17)	122.9(2)
P2–N7	1.661(3)	1.649(3)	O1–P1–N4	100.20(13)	102.09(13)
P1–N4	1.666(3)	1.659(3)	O1–P1–N3	108.98(13)	110.37(15)
P1–O1	1.593(2)	1.590(2)	N1–P1–O1	108.24(14)	107.46(14)

Table 5 — Antimicrobial activities of the free phosphazene bases (**4a–4d** and **5a–5d**) and PMOSs (**6a–6d** and **7a**) expressed as inhibition zones against the five G (+) bacteria (mm)

	Enterococcus faecalis ATCC 29212 G (+)	*Enterococcus hirae* ATCC 9790 G (+)	*Staphylococcus aureus* ATCC 25923 G (+)	*Bacillus subtilis* ATCC 6633 G(+)	*Bacillus cereus* NRRL B-3711 G (+)
Amp	27.0 ± 0.0	9.0 ± 1.0	44.0 ± 1.0	23.0 ± 1.0	-
C	20.0 ± 0.0	22.0 ± 1.0	24.0 ± 1.0	21.0 ± 1.0	-
4	-	-	-	10.5 ± 0.5	10.0 ± 1.0
5	-	-	-	-	-
4b	13.0 ± 0.0	-	-	-	14.7 ± 0.9
5b	-	-	-	-	13.0 ± 0.8
4d	11.0 ± 0.0	-	13.0 ± 0.0	12.5 ± 0.5	13.7 ± 1.2
5d	12.0 ± 0.0	-	-	-	15.0 ± 0.0
4c	-	-	-	12.5 ± 0.5	14.0 ± 1.4
5c	-	-	-	10.0 ± 0.0	15.0 ± 2.2
4a	-	-	10.7± 0.5	20.0 ± 0.0	14.0 ± 1.2
5a	-	-	15.3 ± 0.5	30.3 ± 0.5	30.7 ± 1.7
6a	-	-	11.5 ± 0.5	18.7 ± 1.2	13.0 ± 0.0
6b	-	-	-	17.0 ± 0.8	17.3 ± 0.5
6c	-	-	16.5 ± 0.5	20.3 ± 0.9	15.0 ± 0.8
6d	-	-	-	19.0 ± 1.6	17.0 ± 2.2
7a	-	-	11.0 ± 0.0	30.0 ± 0.0	19.3 ± 1.9

Amp: Ampicillin, C: Chloramphenicol

Table 6 — Antimicrobial activities of the free phosphazene bases (**4a–4d** and **5a–5d**) and PMOSs (**6a–6d** and **7a**) expressed as inhibition zones against the three G (−) bacteria (mm)

	***Proteus vulgaris* RSSK 96029 G (-)**	***Salmonella typhimurium* ATCC 14028 G (-)**	***Klebsiella pneumoniae* ATCC 13883 G (-)**
Amp	-	19.0 ± 1.0	-
C	32.0 ± 1.0	38.0 ± 1.0	31.0 ± 1.0
4	11.3 ± 0.5	14.0 ± 1.0	12.0 ± 0.0
5	15 ± 2.16	-	-
4b	16.5 ± 1.5	14.0 ± 0.0	17.0 ± 0.0
5b	18.3 ± 1.2	14.0 ± 0.0	16.5 ± 0.5
4d	19.0 ± 0.0	14.7 ± 1.2	-
5d	-	15.0 ± 0.0	22.7 ± 4.5
4c	15.3 ± 0.5	14.0 ± 1.0	16.0 ± 0.0
5c	14.0 ± 1.0	-	-
4a	-	14.0 ± 0.0	10.3 ± 0.9
5a	20.3 ± 0.5	-	19.0 ± 0.0
6a	15.5 ± 0.5	17.0 ± 0.0	19.0 ± 0.0
6b	15.0 ± 0.0	-	-
6c	16.7 ± 2.4	16.0 ± 0.8	23.0 ± 0.8
6d	21.7 ± 0.9	15.0 ± 0.0	20.0 ± 0.0
7a	16.0 ± 0.0	17.3 ± 1.2	16.0 ± 1.4

Amp: Ampicillin, C: Chloramphenicol

Table 7 — Antifungal activities of the free phosphazene bases (**4a-4d** and **5a-5d**) and PMOSs (**6a-6d** and **7a**) expressed as inhibition zones against the three fungi (mm)

	Candida albicans ATCC 10231	*Candida topicalis* NRRL-Y-12968	*Candida krusei* ATCC 6258
Keto	11.0 ± 1.0	34.0 ± 2.0	18.0 ± 1.0
4	-	-	-
5	-	-	-
4b	-	-	14.5 ± 0.5
5b	-	-	-
4d	-	-	16.0 ± 0.0
5d	-	11.0 ± 0.0	11.0 ± 0.0
4c	11.0 ± 0.0	-	12.0 ± 0.0
5c	-	-	12.0 ± 0.8
4a	-	11.0 ± 0.9	-
5a	-	-	-
6a	-	-	-
6b	-	15.0 ± 0.0	14.0 ± 0.0
6c	-	-	-
6d	-	-	-
7a	-	-	-

Keto: Ketokanozol

and **6a–6d** are found to very close to reference antibiotics. Compound **5a** is also very active against *B. cereus* G (+). On the other hand, the starting tetrachloro compounds **4** and **5** have the lowest antimicrobial activities against all the G (+) and G (−) pathogenic bacteria. When four Cl atoms were replaced with the secondary amines, the antimicrobial activities of the obtained tetraaminophosphazenes were observed to increase. Among all the compounds, the piperidino phosphazenes have the greatest antimicrobial activities against G (+) bacteria. However, when the activities of the free phosphazene bases (**4a** and **5a**) and their gentisic acid salts (**6a** and **7a**) were compared, it was observed that the activities of these compounds were almost the same. The salts (**6a, 6c, 6d** and **7a**) are slightly more effective than those of the free bases (**4, 4b, 4d** and **5d**) against *S. typhimurium* G (−). Similarly, the piperidino salts (**6a** and **7a**) among the others are the most effective compounds against *S. typhimurium* G (−). The compound **4c** is almost as active as Ketokonazole against to *C. albicans.* The compounds **4b, 4d** and **6b** exhibit moderate antifungal activities against *C. krusei.*

Minimum inhibitory concentrations (MIC), minimum bactericidal and minimal fungicidal concentrations (MBC/MFC) of the cyclotriphosphazenes were determined as well. MIC (Table 8) and MBC/MFC (Table 9) values of the tested compounds were ranged from 62.5 μM (**4a** for *C. tropicalis*) to 2000 μM and 125 μM (**4a** for *C. tropicalis*) to 2000 μM. MIC and MBC/MFC values against *K. pneumoniae* of **5d, 6c** and **7a** are even higher than the MIC and MBC/MFC values of ampicillin and chloramphenicol. Likewise, the MIC and MBC/MFC values against *P. vulgaris* of **5, 4c, 5a, 5b, 6c, 6d** and **7a** are found to be smaller than those of reference antibiotics. Consequently, it is understood that G(+) bacteria are more sensitive to the test samples as compared with G(−) bacteria.

Table 8. — Minimum inhibitory concentrations (MIC, μM) of the compounds against test strains

	Salmonellatyphimurium ATCC 14028 G (−)	*Proteus vulgaris* RSKK 9690 G (−)	*Staphylococcus aureus* ATCC 25923 G (+)	*Bacillus subtilis* ATCC 6633 G (+)	*Bacillus cereus* NRRL B-3711 G (+)	*Klebsiella pneumoniae* ATCC 13883 G (−)	*Candidatropicalis* NRRL Y-12968
Amp	<19.5	1250	<19.5	<19.5	156	1250	
C	156	1250	156	78	156	625	
Keto							78
5		125					
5b		125					
5d					2000	250	
4c		250					
5c					2000		
4a			250	2000	2000		62.5
5a		125	250	2000	2000		
6a				2000			
6b				2000	2000		
6c	250	125		2000	2000	500	
6d		125		2000	2000		
7a	250	125		2000	2000	250	

Amp: Ampicillin, C: Chloramphenicol, Keto: Ketokanozol

Table 9 — Minimum bactericidal and minimal fungicidal concentration (MBC/MFC, μM) of the compounds against test strains

	Salmonellatyphimurium ATCC 14028 G (−)	*Proteus vulgaris* RSKK 9690 G (−)	*Staphylococcus aureus* ATCC 25923 G (+)	*Bacillus subtilis* ATCC 6633 G (+)	*Bacillus cereus* NRRL B-3711 G (+)	*Klebsiella pneumoniae* ATCC 13883 G (−)	*Candidatropicalis* NRRL Y-12968
Amp	<19.5	2500	<19.5	<19.5	2500	1250	
C	1250	2500	2500	78	1250	2500	
Keto							1250
5		250					
5b		250					
5d					2000	500	
4c		500					
5c					2000		
4a			500	2000	2000		125
5a		250	500	2000	2000		
6a				2000			
6b				2000	2000		
6c	500	250		2000	2000	500	
6d		250		2000	2000		
7a	500	250		2000	2000	500	

Amp: Ampicillin, C: Chloramphenicol, Keto: Ketokanozol

On the other hand, the pyrrolidino- and piperidino-cyclotriphosphazenes carrying 4-fluoro-benzyl-N/N[59] and ferrocenyl-N/N-spirocyclic groups[60] were found to be active against *E. coli, S. aureus, B. cereus* and *B. subtilis* bacteria, and *C. albicans* and *C. tropicalis* fungi. Whereas, tetra-morpholino and 1,4-dioxa-8-azaspiro[4,5]deca-4-fluoro-benzyl-N/N-cyclotriphosphazene derivatives did not have a significant effect on these bacteria.[12] However, analogous compounds; pyrrolidino-, piperidino-, morpholino and 1,4-dioxa-8-azaspiro[4,5]deca- 4-fluoro-benzyl-N/O-spiro-cyclic cyclotriphosphazenes were found to be significantly active against *C. Albicans*.[10] In fact, these compounds can be considered as anticandidal agents. It is reported that although the antifungal activities of the salts (PMOSs) of these compounds decrease against *C. albicans*, the antimicrobial activities against *E. fecalis* and *E. coli* increase.[29] As a result, the antimicrobial activities of the aminocyclotriphosphazenes and phosphazenium

salts appear to be largely dependent on the occurrences of the hydrogen bonds with the ligands attached to the phosphorus atoms and the active centres of microorganism cell components.

Interaction with plasmid DNA and restriction enzyme digestion

Interactions with plasmid DNA at four different concentrations of 2000, 1000, 500 and 250 μM according to the decreasing concentrations of the compounds prepared in 2000 μM concentrations dissolved in DMF (dimethylformamide) were elucidated (Fig. 5). The cleavage studies of supercoiled plasmid DNA were carried out using agarose gel electrophoresis. After binding of the cyclotriphosphazenes to plasmid DNA at different molar ratios, the changes in electrophoretic mobilities of the open circular (oc, relaxed) and closed circular (cc, supercoiled) forms were analyzed (Fig. 5).

In general, two DNA bands; Forms I (strong) and II (weak), appeared in both untreated and treated plasmid DNA. When the concentration of the cyclotriphosphazenes increases, the mobilities of Forms I and II plasmid DNA decreases in the case of **4** and **5**. All three forms were observed for **4** and **5** as a result of a 24 h incubation. In the case of **4b** and **5b**, the mobilities of Forms I and II decrease. In the case of **5c**, a coalesced band was observed in Lanes 1 and 2. In the case of the other compounds, no changes in the mobilities of Forms I and II DNA bands were observed. The changes in the mobilities of the bands display changes in DNA conformations by covalent binding of the compounds with the DNA.

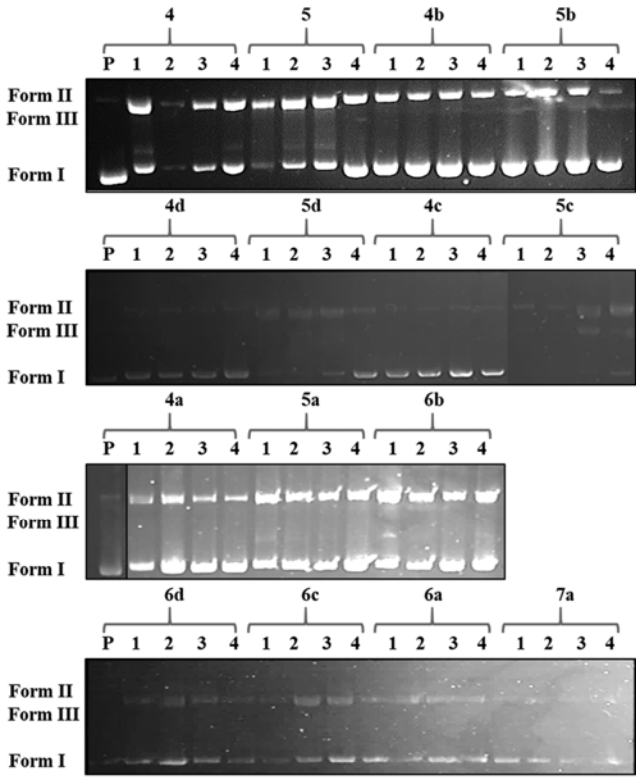

Fig. 5 — Modification of gel electrophoretic mobility of plasmid DNA when incubated with various concentrations of the compounds. Concentrations are as follows: (P) untreated plasmid DNA; for compounds: (line 1) 2000; (line 2) 1000; (line 3) 500 and (line 4) 250 μM. The top and the bottom bands correspond to form II (open circular) and form I (covalently closed circular) plasmids, respectively

BamHI and HindIII digestions of the compounds-plasmid DNA mixture

To understand more about changes in DNA conformation, compound-DNA incubation monitored by *Bam*HI and *Hind*III digestions were used. The electrophoretogram corresponding to the *Bam*HI and *Hind*III digested incubated mixtures of pBR322 plasmid DNA, and the free phosphazene bases (**4a-4d** and **5a-5d**) and PMOSs (**6a-6d** and **7a**) are shown in Fig. 6. These compounds inhibited restriction enzyme digestion. Untreated pBR322 plasmid DNA is applied to Lane P. Lane P/B and Lane P/H are placed to plasmid DNA digested with *Bam*HI and *Hind*III, respectively. *Bam*HI enzyme binds at the sequence 5'-G/GATCC-3' and since pBR322 plasmid DNA contains a single sequence of that, cleaves this sequence. *Bam*HI then converts supercoiled Form I and open circular Form II to linear form of linear DNA (Form III). *Hind*III recognizes the sequence 5'-A/AGCTT-3' and cleaves this sequence. So, *Hind*III converts Forms I and II to Form III similarly to *Bam*HI. As a result, the treatment of the compounds with the *Hind*III enzyme only the compound **5c** was not cleaved. That is, **5c** binds to the DNA through the 5'A/AGCTT-3 ' nucleotide sequence.

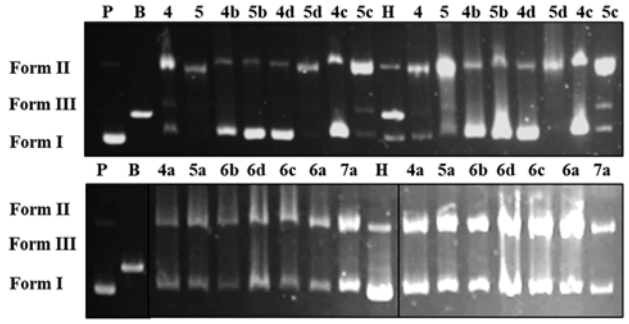

Fig. 6 — Electrophoretograms applying to incubated mixtures of plasmid DNA and the compounds followed by digestion with *BamH*I and *Hind*III. Lane P corresponds to the untreated and indigested plasmid DNA. Lane B and Lane H apply to untreated but digestion with *BamH*I and *Hind*III, respectively

Table 10 — % Viability of the L929 fibroblast cancer cells exposed to concentrations of 12.5-100 µg/mL of the compounds for 24 h by WST Assay. The cell viability (%) based on mean absorbance values at 440 nm is presented (Data are expressed as a mean ± standard error as calculated from 3 separate experiments)

	6d	**6b**	**6a**	**Doxorubicin***
100 µg/mL	117.5	89.2	82.5	39.2
50 µg/mL	115.5	134	123.4	40.8
25 µg/mL	122.6	113.1	154.1	51.1
12.5 µg/mL	119.6	95.4	171.5	57.7

*Cell viability of the control group (an only medium) is 100% for L929 fibroblast cells

Table 11 — % Viability of MDA-MB-231 breast cancer cells exposed to concentrations of 12.5-100 µg/mL of the compounds for 24 h by WST Assay. The cell viability (%) based on mean absorbance values at 440 nm is presented (data are expressed as a mean ± standard error as calculated from 3 separate experiments)

	6d	**6b**	**6a**	**Doxorubicin***
100 µg/mL	66.85	78.60	51.54	24.62
50 µg/mL	72.48	81.17	67.95	39.94
25 µg/mL	77.62	80.44	66.60	42.54
12.5 µg/mL	80.07	82.03	71.25	45.10

*Cell viability of the control group (an only medium) is 100% for MDA-MB-231 breast cancer cell lines

Cytotoxicity of the compounds on L929 fibroblast and MDA-MB-231 breast cancer cells

The cytotoxic activities of the PMOSs (**6a, 6b** and **6d**) were evaluated using WST-1 assay against L929 healthy fibroblasts (mouse cells) and MDA-MB-231 breast cancer cell lines. The percentages of viable cells were figured out at various concentrations (12.5–100 µg/mL) against % cell viability (Tables 10 and 11). In terms of WST-1 results, the highest cytotoxic effect is observed for **6b** at the lowest concentration (12.5 µg/mL) against fibroblast cell line. Whilst, the compounds **6a** and **6d** in the same experimental condition have slightly and moderately cytotoxic effect on the L929 fibroblast cell line, respectively. The highest cytotoxic effect is found to be for the tetrapiperidino salt **6a** against to the MDA-MB-231 breast cancer cell line, and while the moderate effect is observed for the tetraDASD substituted salt **6d**.

Consequently, the compound **6a** exhibited strong anticancer activity against MDA-MB-231 breast cancer cells. IC50 values of **6a** for L929 fibroblast and MDA-MB-231 cells were lower than 100 µg/mL. The anticancer activity of **6a** was as effective as anticancer activity of doxorubicin on the MDA-MB-231 breast cancer cell line. However, due to the lowest toxic activity of this compound against fibroblast cell as well, indicating that it may be a promising the anticancer drug candidate for *in vivo* experiments on account of its selective feature. On the other hand, the tetra-chloro/piperidino-4-fluoro-benzyl-N/O,[10] and the tetramorpholino-4-fluoro-benzyl-N/N[12] phosphazenes were referred to have cytotoxic activities against MCF-7 breast and Hela cancer cell lines, respectively. Besides, the tetra-pyrrolidino/piperidino-4-fluoro-benzyl-N/N phosphazenium salts also exhibit anticancer activities against DLD-1 colon cancer cells.[30]

Antituberculosis activity

In vitro antituberculosis activities of the free phosphazene bases (**4a-4d** and **5a-5d**) and PMOSs (**6a-6d** and **7a**) were evaluated against *M. tuberculosis* H37Rv reference strain using the agar proportion method (CLSI).[47,48] After 21 days incubation, the susceptibility results of the cyclotriphosphazenes displayed that the tested compounds did not exhibit any activities against *M. tuberculosis* H37Rv strain.

Conclusions

In conclusion, the preparations of the new gentisic acid PMOSs containing 2-pyridyl pendant arm (**6a-6d** and **7a**) were presented and whose structures were evaluated by various spectroscopic and crystallographic techniques, and scrutinized for their biological activities in cultured cell lines. The X-ray crystallographic results exhibit that **6c** is protonated with the N of the phosphazene ring near to the N/O spiro ring. This compound has chirality, and the absolute configuration of P1 center is found to be as R in the solid state. But, in the $CDCl_3$ solution, the proton is replaced between the nitrogen atoms, and so the chirality disappeared. It is noteworthy that this result is observed in the phosphazenium salts for the first time. According to these findings, all the PMOSs ought to have chiralities in the solid state. The

characteristic ^{31}P NMR spectrum of **6c** was recorded in the range of (−28) – (+25) °C, and no changes were observed in AB_2 spin system. Taking into account of this finding, one can say that the other PMOSs (**6a-6d** and **7a**) may also have chiral properties in the solid state, but not in $CDCl_3$ solution. The spectrum of **6c** is used as a guide to assign the ^{31}P NMR spectra of the other PMOSs. On the other hand, the thermal analysis results indicate that **6a, 6b** and **7a** decompose at lower temperatures than the other PMOSs (**6c** and **6d**), and thermal stability (788 °C) of **7a,** which has an N/N spiro ring is lower than those of the others. Besides, PMOS **6c** can be used as an ionic liquid according to the thermoanalytical data. In addition, the antimicrobial activity results show that the piperidino phosphazenes have the greatest antimicrobial activities against G (+) bacteria. According to the cytotoxicity results, PMOS **6a** has strong anticancer activity against MDA-MB-231 breast cancer cells compared to the other phosphazenium salts. However, since this salt exhibits very low toxicity against the healthy fibroblast cells, further studies ought to be made to use it as an anticancer drug candidate in *in vivo* experiments.

Supplementary Data

Listings of The ESI-MS spectrum of **5a (**Fig. S1), the ^{13}C and ^{1}H NMR spectra of **6a** (Figs. S2 and S3), the second order effect in ^{13}C $\{^{1}H\}$ NMR spectrum of **6b** (Fig. S4), TG curves of the phosphazenium salts **(6a-6d** and **7a)** (Fig. S5), the shapes of the trimeric phosphazene rings in **4a** and **6c** with torsion angles (deg) given (Fig. S6), the conformations of (a) the trimeric phosphazene ring and (b) the six-membered spiro-ring of **4a** (Fig. S7), the conformations of (a) the trimeric phosphazene ring and (b) the six-membered spiro-ring of **6c** (Fig. S8), hydrogen-bond geometries for **6c** (Table S1) and the packing diagram of **6c** (Fig. S9). Supplementary data is available in the electronic form at http://www.niscair.res.in/jinfo/ijca/IJCA_56A(04)533-550_SupplData.pdf.

Acknowledgement

The authors thank the "Scientific and Technical Research Council of Turkey" (Grant No. 216Z105). T. H. is grateful to Hacettepe University Scientific Research Project Unit (Grant No. 013 D04 602 004), and Z. K. thanks to the Turkish Academy of Sciences (TÜBA) for partial support of this work.

References

1 Stewart F F, *Organophosphorus Chem,* (Cambridge, UK: Royal Society of Chemistry), 44 **(**2015) 397.
2 Chandrasekhar V & Narayanan R S, *Organophosphorus Chem,* (Cambridge, UK: Royal Society of Chemistry), 45 (2016) 375.
3 Chandrasekhar V & Narayanan R S, *Organophosphorus Chem,* (Cambridge, UK: Royal Society of Chemistry), 46 (2017) 342.
4 Chandrasekhar V & Chakraborty A, *Organophosphorus Chem,* (Cambridge, UK: Royal Society of Chemistry), 48 (2019) 400.
5 Yıldız M, Kılıç Z & Hökelek T, *J Mol Struct,* 510 (1999) 227.
6 İlter E E, Asmafiliz N, Kılıç Z, Işıklan M, Hökelek T, Çaylak N & Şahin E, *Inorg Chem,* 46 (2007) 9931.
7 Allen C W, *Chem Rev,* 91 (1991) 119.
8 Keshav K, Singh N & Elias AJ, *Inorg Chem,* 49 (2010) 5753.
9 Okumuş A, Akbaş H, Kılıç Z, Koç L Y, Açık L, Aydın B, Türk M, Hökelek T & Dal H, *Res Chem Intermed,* 42 (2016) 4221.
10 Okumuş A, Elmas G, Kılıç Z, Ramazanoğlu N, Açık L, Türk M & Akça G, *Turk J Chem,* 41 (2017) 525.
11 Tümer Y, Asmafiliz N, Kılıç Z, Hökelek T, Koç L Y, Açık L, Yola M L, Solak A O, Öner Y, Dündar D & Yavuz M, *J Mol Struct,* 1049 (2013) 112.
12 Akbaş H, Okumuş A, Kılıç Z, Hökelek T, Süzen Y, Koç L Y, Açık L & Çelik Z B, *Eur J Med Chem,* 70 (2013) 294.
13 Jimenez J, Laguna A, Gascon E, Sanz J A, Serrano J L, Barbera J & Oriol L, *Chem Eur J,* 18 (2012) 16801.
14 Jimenez J, Pintre I, Gascon E, Sanchez-Somolinos C, Alcala R, Cavero E, Serrano J L & Oriol L, *Macromol Chem Phys,* 215 (2014) 1551.
15 Omotowa B A, Phillips B S, Zabinski J S & Shreeve J M, *Inorg Chem,* 43 (2004) 5466
16 Greaves T L & Drummond C J, *Chem Rev,* 108 (2008) 206.
17 Schrogel P, Hoping M, Kowalsky W, Hunze A, Wagenblast G, Lennartz C & Strohriegl P, *Chem Mater,* 23 (2011) 4947.
18 Nishimoto T, Yasuda T, Lee S Y, Kondo R & Adachi C, *Mater Horiz,* 1 (2014) 264.
19 Harrup M K, Gering K L, Rollins H W, Sazhin S V, Benson M T, Jamison D K, Michelbacher C J & Luther T A, *ESC Trans,* 41 (2012) 13.
20 Xu R & Xu Y, *Mod Inorg Synth Chem,* 11 (2017) 295.
21 Greish Y E, Bender J D, Lakshmi S, Brown P W, Allcock H R & Laurencin C T, *Biomaterials,* 26 (2005) 1.
22 Lakshmikandhan T, Sethuraman K, Chandramohan A & Alagar M, *Polym Compos,* 38 (2017) 24.
23 Elmas G, Okumuş A, Cemaloğlu R, Kılıç Z, Çelik S P, Açık L, Tunalı B Ç, Türk M, Çerçi N A, Güzel R & Hökelek T, *J Organomet Chem,* 853 (2017) 93.
24 Siwy M, Sęk D, Kaczmarczyk B, Jaroszewicz I, Nasulewicz A, Pelczyñska M, Nevozhay D & Opolski A, *J Med Chem,* 49 (2006) 806.
25 Elmas G, Okumuş A, Kılıç Z, Çam M, Açık L & Hökelek T, *Inorg Chim Acta,* 476 (2018) 110.
26 Karadağ A & Akbaş H, *Recent Advances in Ionic Liquids,* (Intech Open) 2018
27 Allcock H R, *Chem Rev,* 72 (1972) 315.
28 Elmas G, Okumuş A, Kılıç Z, Gönder L Y, Açık L & Hökelek T, *J Turk Chem Soc Sect A: Chem,* 3 (2016) 25.

29 Elmas G, Okumuş A, Kılıç Z, Çelik S P & Açık L, *J Turk Chem Soc Sect A: Chem,* 4 (2017) 993.

30 Akbaş H, Okumuş A, Karadağ A, Kılıç Z, Hökelek T, Süzen Y, Koç L Y, Açık L, Aydın B & Türk M, *J Therm Anal Calorim,* 123 (2016) 1627.

31 Akbaş H, Karadağ A, Aydın A, Destegül A & Kılıç Z, *J Mol Liq,* 230 (2017) 482.

32 Coles S J, Davies D B, Eaton R J, Hursthouse M B, Kılıç A, Mayer T A, Shaw R A & Yenilmez G, *J Chem Soc Dalton Trans,* (2002) 365.

33 Beşli S, Coles S J, Davies D B, Eaton R J, Hursthouse M B, Kılıç A, Shaw R A, Çiftçi G Y & Yeşilot S, *J Am Chem Soc,* 125 (2003) 4943.

34 Binici A, Okumuş A, Elmas G, Kılıç Z, Ramazanoğlu N, Açık L, Şimşek H, Tunalı B Ç, Türk M, Güzel R & Hökelek T, *New J Chem,* 43 (2019) 6856.

35 Elmas G, *J Turk Chem Soc Sect A: Chem,* 5 (2018) 621.

36 Elmas G, *Phosphorus Sulfur Silicon Relat Elem,* 194 (2019) 13.

37 Bruker program 1D WIN-NMR (release 60) and 2D WIN-NMR (release 61).

38 Bruker SADABS, Bruker AXS Inc Madison, Wisconsin, USA 2005.

39 Sheldrick M, *SHELXS*-97, *SHELXL*-97 (University of Gottingen, Gottingen, Germany) 1997.

40 Sheldrick G M, *Acta Crystallogr Sect A,* 64 (2008) 112.

41 Hongyan L, Lo J M, Fanwick P E, Stowell J G & Green M A, *Inorg Chem,* 38 (1999) 2071.

42 Perez C, Pauli M & Bazerque P, *Acta Biol Med Exp,* 15 (1990) 113.

43 Elmas G, Okumuş A, Sevinç P, Kılıç Z, Açık L, Atalan M, Türk M, Deniz G & Hökelek T, *New J Chem,* 41 (2017) 5818.

44 Sambrook J, Fritsch E F & Maniatis T, Molecular cloning:a laboratory manual *Cold Spring Harbor*, (New York) 1989.

45 Okumuş A, Elmas G, Cemaloğlu R, Aydın B, Binici A, Şimşek H, Açık L, Türk M, Güzel R, Kılıç Z & Hökelek T, *New J Chem*, 40 (2016) 5588.

46 Rzayev Z M O, Türk M & Söylemez E A, *Bioorg Med Chem,* 20 (2012) 5053.

47 Antimycobacterial susceptibility testing for Mycobacterium tuberculosis, Tentative standard M24-T, National Committee for Clinical Laboratory Standards (NCCLS), (Wayne, PA) 1995.

48 Susceptibility testing of mycobacteria, nocardia, and other aerobic actinomycetes, Approved standard M24-A, National Committee for Clinical Laboratory Standards (NCCLS), (Wayne, PA) 2003.

49 Pidcock E, *Chem Commun,* (2005) 3457.

50 Dey A & Pidcock E, *CrystEngComm,* 10 (2008) 1258.

51 Carriedo G A, Alonso F G, Gonzalez P A & Menendez J R, *J Raman Spectrosc,* 29 (1998) 327.

52 Elmas G, *Phosphorus Sulfur Silicon Relat Elem,* 192 (2017) 1224.

53 Krishnadevi K, Selvaraj V & Prasanna D, *RSC Adv,* 5 (2015) 913.

54 Liu R & Wang X, *Polym Degrad Stabil,* 94 (2009) 617.

55 Cremer D & Pople J A, *J Am Chem Soc,* 97 (1975) 1354.

56 Farrugia L J, *J Appl Cryst,* 30 (1997) 565.

57 Farrugia L J, *J Appl Cryst,* 45 (2012) 849.

58 Krishnadevi K & Selvaraj V, *Appl Surf Sci,* 366 (2016) 148.

59 Okumuş A, Kılıç Z, Hökelek T, Dal H, Açık L, Öner Y & Koç L Y, *Polyhedron,* 30 (2011) 2896.

60 Asmafiliz N, Kılıç Z, Öztürk A, Süzen Y, Hökelek T, Açık L, Çelik Z B, Koç L Y, Yola M L & Üstündağ Z, *Phosphorus Sulfur Silicon Relat Elem,* 188 (2013) 1723.